EUROPEAN ORGANIZATION FOR NUCLEAR RESEARCH

CERN-PPE/90-146
2 October 1990

Hyperon-Antihyperon Production at LEAR

Tord Johansson
Dept. of Radiation Sciences, Uppsala University
Box 535, S-75121 Uppsala, Sweden

representing the PS185 Collaboration:

P.D. Barnes[1], P. Birien[4], W.H. Breunlich[8], G Diebold[1], W. Dutty[4], R.A. Eisenstein[5], W. Eyrich[3], H.Fischer[4], R. von Frankenberg[6], G. Franklin[1], J. Franz[4], R. Geyer[8], N. Hamann[2], D. Hertzog[5], T. Johansson[7], K. Kilian[6], M. Kirsch[3], R. Kraft[3], C. Maher[1], D. Malz[3], W. Oelert[6], S. Ohlsson[7], B. Quinn[1], E. Rössle[4], H. Schledermann[4], H. Schmitt[4], R. Schumacher[1], T. Sefzick[6], G.Sehl[6], J. Seydoux[1], F. Stinzing[3], R. Tayloe[5], R. Todenhagen[4] and M. Ziolkowski[6]

1) Carnegie Mellon University, Pittsburgh PA, USA
2) CERN, Geneva, Switzerland
3) University of Erlangen-Nürnberg, Erlangen, Fed. Rep. Germany
4) University of Freiburg, Freiburg, Fed. Rep. Germany
5) University of Illinois, Urbana IL, USA
6) Institut für Kernphysik der KFA, Jülich, Fed. Rep. Germany
7) Uppsala University, Sweden
8) Institut für Mittelenergiephysik der ÖAW, Vienna, Austria

ABSTRACT

The PS185 collaboration studies the production of antihyperon-hyperon pairs in antiproton-proton collisions at LEAR in the threshold region. Results obtained for the reactions $\bar{p}p \rightarrow \bar{\Lambda}\Lambda$ and $\bar{p}p \rightarrow \bar{\Lambda}\Sigma^0$+ c.c. are shown and discussed. They include total and differential cross sections as well as polarisations. For the $\bar{\Lambda}\Lambda$ channel spin-correlations are obtained as well.

Invited talk given at the First Biennial Conference on Low Energy Antiproton Physics, Stockholm, Sweden, 2 - 6 July 1990, to appear in the Proceedings.

1. INTRODUCTION

The study of production of antihyperon-hyperon pairs in $\bar{p}p$ collisions close to the reaction threshold has been motivated by the prospect of learning about the underlying strangeness exchange process. The threshold region is of particular interest in this context since the number of partial waves involved is small. Observables such as angular distributions, polarisations and spin-correlations can be used to extract information about the underlying dynamical processes. The PS185 collaboration has produced high-quality data on these quantities from the reactions $\bar{p}p \rightarrow \bar{\Lambda}\Lambda$ and $\bar{p}p \rightarrow \bar{\Lambda}\Sigma^0$+ c.c. [1-8].

In the constituent quark model, this strangeness exchange process is governed by the annihilation of a $\bar{q}q$-pair and the subsequent creation of an $\bar{s}s$-pair (Fig. 1a). Here, the non-participating spectator quarks form an I = S = 0 di-quark in the Λ case, whereas they have I = S = 1 in the Σ^0 case. Therefore, in this model the spin of the Λ is carried by the strange quark and the spin observables will reflect the reaction dynamics. Calculations based on this model are often labelled $^3P_0$ or $^3S_1$ depending on whether the $\bar{s}s$-pair is created with gluon or vacuum quantum numbers respectively [9-17]. Alternatively, the process can also be described in a conventional t-channel boson-exchange model in which kaons are exchanged (Fig. 1b). The relative importance of the exchange of different K-mesons varies between the models [18-26].

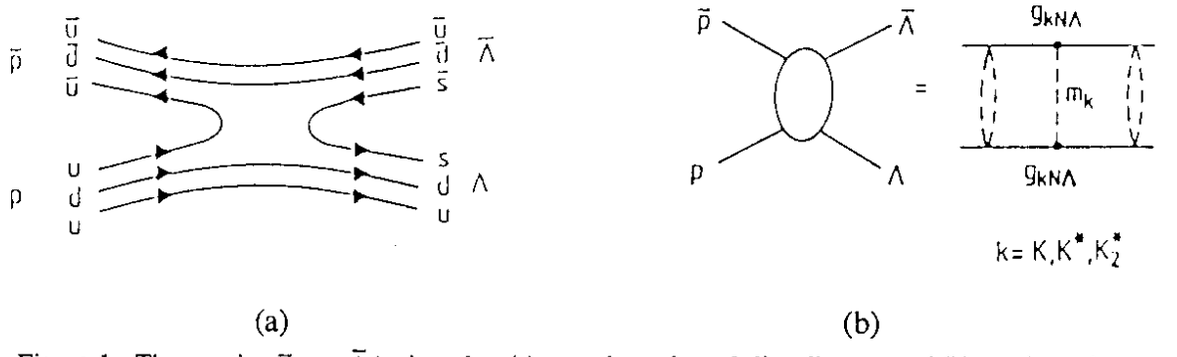

Figure 1. The reaction $\bar{p}p \rightarrow \bar{\Lambda}\Lambda$ viewed as (a) an s-channel quark-line diagram and (b) a t-channel meson exchange.

Neither the constituent quark model nor the kaon-exchange model can produce polarisation in the final state without the inclusion of initial and final state interactions. Experimental data are available for the $\bar{p}p$ interaction in the energy domain of interest and therefore constrain the $\bar{p}p$ optical potential used. However, nothing is known experimentally about the antihyperon-hyperon interaction, leaving much freedom, in particular for the annihilation part, in the choice of the parameters of the $\bar{Y}Y$ potential.

The theoretical work has so far concentrated on the channel $\bar{p}p \rightarrow \bar{\Lambda}\Lambda$, where data have been available. Both approaches are rather successful in describing differential cross sections and polarisations. In fact, the quark and the boson-exchange approaches give very similar results, perhaps reflecting the liberty in fitting the potential parameters. In this context the reaction $\bar{p}p \rightarrow \bar{\Lambda}\Sigma^0$+ c. c. is of particular interest. The long-ranged

K(494) exchange is suppressed here: SU(3) relations give the ratio of the coupling constants $g^2_{KN\Sigma^0}/g^2_{KN\Lambda} = 1/27$. As a consequence the more short-ranged $K^*(892)$ exchange becomes more important for the $\bar{\Lambda}\Sigma^0$ reaction since $g^2_{K^*N\Sigma^0}/g^2_{K^*N\Lambda} \approx 0.8$, and one might hope that the reaction dynamics would be more sensitive to quark effects [13]. More details on the quark-based model and on the boson exchange model are given in contributions by M. Alberg and by P. La France in these proceedings.

It has been argued that due to the large mass difference between the annihilated $\bar{q}q$-pair and the created $\bar{s}s$-pair these processes might be treated perturbatively [9, 10]. Ratios of cross sections between different hyperon channels can then be predicted under the assumption that the non-perturbative effects (*i.e.*, initial and final state interactions) will cancel, provided that the comparison is made under the correct kinematical conditions.

2. EXPERIMENT

The PS185 detector is a forward decay spectrometer as shown in Fig. 2 and is designed particularly for the kinematics of the $\bar{p}p \rightarrow \bar{Y}Y$ reaction. It consists of four principal components: a trigger-active target system consisting of four CH_2 and one carbon cell sandwiched between and surrounded by veto scintillators, a track reconstructing system made out of a stack of 10 multiwire proportional chambers and 13 drift chambers, two scintillator hodoscopes for trigger purposes, and a solenoidal magnet with three drift chambers for baryon number identification. The arrangement is described in more detail in refs.[1,2,27,28].

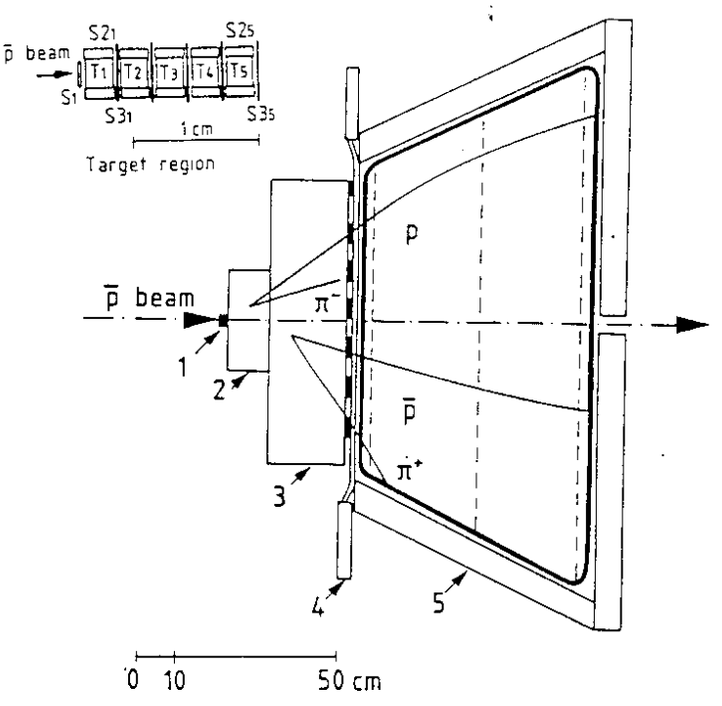

Figure 2. The PS185 experimental setup together with an expanded view of the target region: 1 = target, 2 = multiwire proportional chambers, 3= drift chambers, 4 = scintillator hodoscope, 5 = magnetic solenoid with drift chambers. The toplogy of a $\bar{p}p \rightarrow \bar{\Lambda}\Lambda$ event is indicated.

The hyperon events are identified from their charged delayed decay Y-> Nπ. Due to the threshold kinematics the apparatus, covering only ± 41 degrees in the laboratory system, has in principle a 100% acceptance for the decay baryons for all hyperon channels within the LEAR range ($p_{\bar{p}} < 2$ GeV/c). It is worthwhile to notice the small size of the target cells; they are cylinders of 2.5 mm thickness and 2.5 mm diameter. The LEAR antiproton beam is focussed to a spot of < $1mm^2$ onto the target arrangement in which the ^{12}C cell is used to correct for events coming from the carbon content of the CH_2 cells.

The two-body kinematics allows for a complete kinematical reconstruction of the events in a non-magnetic detector; the information coming from the bending of the particles in the magnet is primarily used to assign the baryon number to the hyperons. The data evaluation is restricted to events having two neutral vees in the chamber stack. After applying geometrical and kinematical cuts, the event candidates are fed into a kinematic fitting procedure for the final analysis. The global efficiency in reconstructing a $\bar{\Lambda}\Lambda$ pair decaying into charged particles, taking into account geometrical and reconstruction efficiencies, is about 60%.

3. RESULTS

3.1 Total Cross Sections

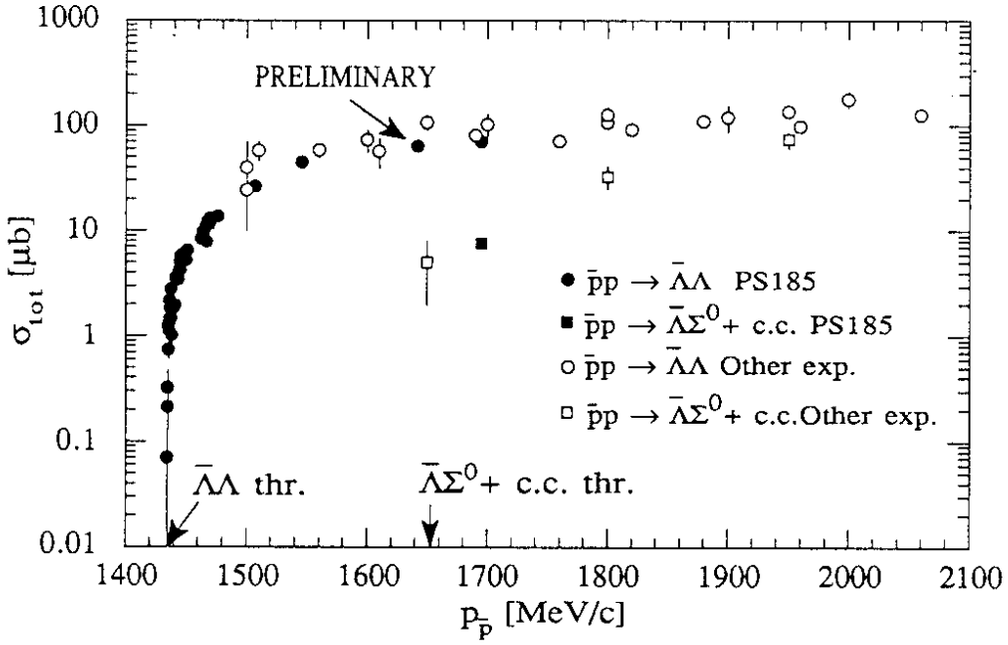

Figure 3. Compilation of available data on $\bar{p}p$ -> $\bar{\Lambda}\Lambda$ and $\bar{p}p$ -> $\bar{\Lambda}\Sigma^0$+ c. c. in the momentum range of LEAR [1-7,29-33]. The threshold momenta p_{thr} ($\bar{\Lambda}\Lambda$) = 1.435 GeV/c, p_{thr} ($\bar{\Lambda}\Sigma^0$+c.c.) = 1.653 GeV/c are indicated with arrows.

The measured excitation function for the reaction measured by PS185 is shown in Fig. 3 [1,2,4,5] together with older data points [29-33]. The corresponding plot for the channel $\bar{p}p \rightarrow \bar{\Lambda}\Sigma^0$+ c.c. including a new PS185 point [3] is also shown. As can be seen, the threshold behaviour for the $\bar{\Lambda}\Lambda$ channel is well mapped out. An expanded view of the region very close to the threshold is shown in Fig. 4. Here for each incoming antiproton momentum there are four data points. They correspond to the four individual CH_2 cells in the target arrangement (see Fig. 2) and the steps downward in energy for the three lower momenta come from the energy loss of the antiprotons in the preceding cells (0.8 MeV/c). New preliminary data points [7] are shown in this figure together with already published ones [2]. These new points contain a lower number of events with respect to the older ones, and the data were taken with a non-optimized experimental setup for $\bar{\Lambda}\Lambda$ threshold studies.

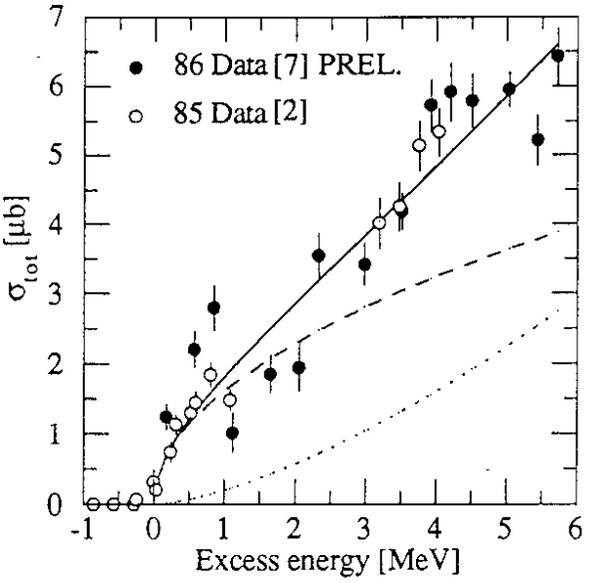

Figure 4. Close to threshold behaviour of the $\bar{p}p \rightarrow \bar{\Lambda}\Lambda$ reaction. The solid curve is a fit to the data (see text). The dashed and dotted curves correspond to the s- ans p-wave contributions to the fit respectively.

Assuming a constant transition matrix element close to threshold, the energy dependence of σ_{tot} only depends on the angular momentum l according to $\sigma_{tot} = b_l \varepsilon^{l+1/2}$. A fit to the data is shown in the figure and gives the values $b_0 = (1.62 \pm 0.08)$ μb/MeV$^{1/2}$ and $b_1 = (0.20 \pm 0.02)$ μb/MeV$^{3/2}$, where ε is the excess energy ($\varepsilon = \sqrt{s} - 2m_\Lambda$). This clearly shows the need to include $l \geq 1$ partial waves already very close to the reaction threshold.

The new data point on the reaction $\bar{p}p \rightarrow \bar{\Lambda}\Sigma^0$+ c.c. allows for a comparison with predicted ratios of cross sections from the constituent quark models. This comparison can be made either at the same $\bar{p}$ momentum or at the same excess energy, and this is done in Table 1.The predicted ratios are a factor of five too large at 1.695 GeV/c. Taking the difference in phase space into account gives a factor of 2.3, but still the predicted ratio is in disagreement by a factor of two. Being relatively close to the $\bar{\Lambda}\Sigma^0$ threshold, a more sensible comparison can be made at the same excess energy for the two reaction channels. In such a way the final state interaction of the outgoing antihyperon-hyperon pair would be better compensated for by taking the ratio of cross sections.

Comparing with a $\bar{\Lambda}\Lambda$ data point at practically the same excess energy, this ratio becomes remarkably close to the theoretical predictions. The difference in phase space in this latter case is a 10% effect.

Table 1. The experimental ratio $\sigma(\bar{\Lambda}\Sigma^0)/\sigma(\bar{\Lambda}\Lambda)$ compared with theoretical predictions ($\sigma(\bar{\Lambda}\Sigma^0)$ = $\sigma(\bar{\Lambda}\Sigma^0$+ c.c.)/2 has been used).

$\sigma(\bar{\Lambda}\Sigma^0)/\sigma(\bar{\Lambda}\Lambda)$	**Reference**
Experiment: 0.054 ± 0.003	PS185: $p_{\bar{p}}$ = 1.695 GeV/c [3,5]
0.132 ± 0.007	" " ,phase space corrected
0.29 ± 0.02	PS185: $\varepsilon \approx 14.7$ MeV [1,3]
Theory:	H. Genz and S. Tatur [9]
0.259	S. Fururi and A. Faessler [14]
	M. Kohno and W. Weise [11]
0.236	H. Rubinstein and H. Snellman [10]

3.2 Differential Cross Sections

Differential cross sections extracted at different momenta for the reaction $\bar{p}p \rightarrow \bar{\Lambda}\Lambda$ are shown in Fig. 5a as a function of the reduced four-momentum transfer t'. A general trend can be seen from the data: a forward peaking of the differential cross section and a flat distribution at larger momentum transfers. This peaking becomes more pronounced at higher momenta, but even very close to the reaction threshold there is a clear anisotropy in the angular distribution [2]. This again emphasizes the importance of partial waves with $l \geq 0$ very close the the kinematical threshold.

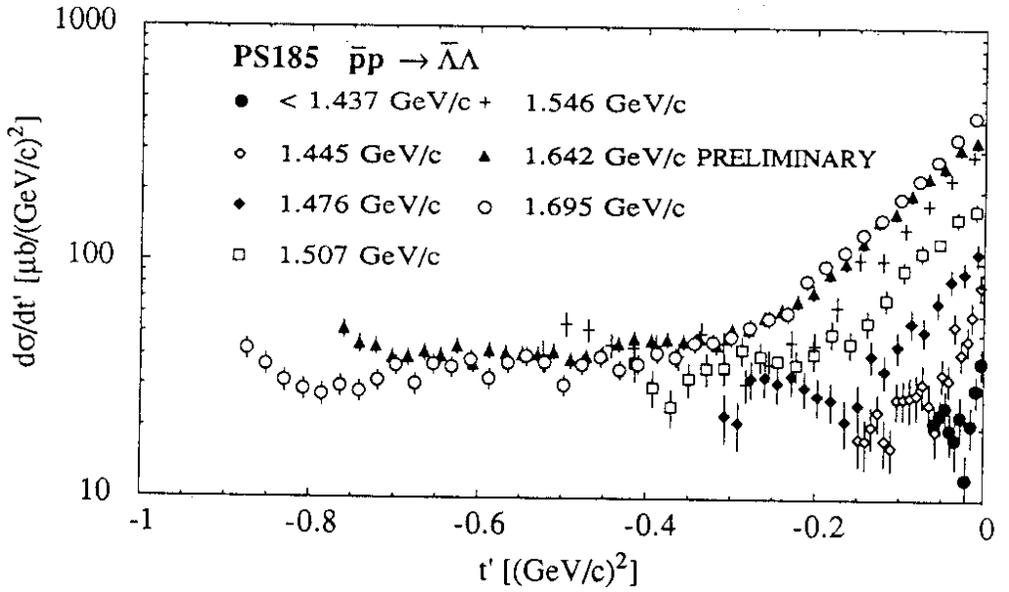

Figure 5a. Differential cross sections as a function of t' for the reaction $\bar{p}p \rightarrow \bar{\Lambda}\Lambda$.

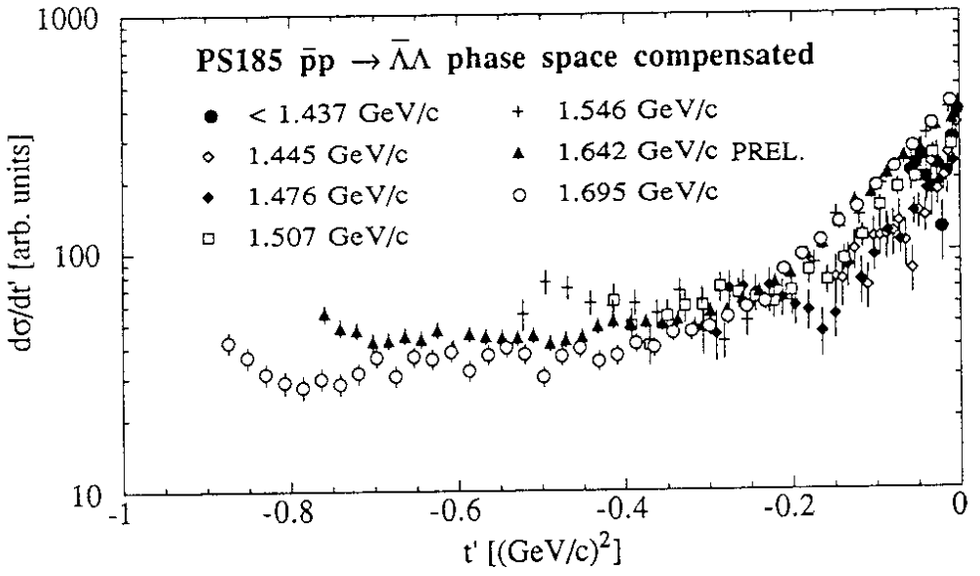

Figure 5b. Differential cross sections as a function of t' for the reaction $\bar{p}p$ -> $\bar{\Lambda}\Lambda$ compensated for the difference in phase space.

In Fig. 5b the same data are plotted compensated for the difference in phase space and normalised at 1.695 GeV/c. Some general features can be seen here: the slope of the forward peak is roughly the same, it varies slowly from 9.6 $(GeV/c)^{-2}$ at 1445 MeV/c to 8.7 $(GeV/c)^{-2}$ at 1695 MeV/c for $|t'| < .15$ $(GeV/c)^2$. We may write in analogy with absorptive scattering:

$$\frac{d\sigma}{dt'} = \left.\frac{d\sigma}{dt'}\right|_{t'=0} e^{-bt'}$$

where the slope parameter may be associated with an absorbing hadronic disc having a radius $R = \sqrt{4b}$. Using the average value 9.1 $(GeV/c)^{-2}$ for b, an absorbtion radius of 1.2 fm is deduced. Another feature of these distributions is that the change from forward rise to a flat distribution occurs at a $t' \approx -.2$ $(GeV/c)^2$ after which the distributions converge. In fact, the data taken at different momenta become very similar when the difference in phase space is accounted for.

The differential cross section for the reaction $\bar{p}p$ -> $\bar{\Lambda}\Sigma^0$+ c.c. has been extracted at $p_{\bar{p}}$ = 1.695 GeV/c [3] and is shown in Fig. 6. As mentioned in the introduction, this reaction channel should be more sensitive to short range effects. The features from the $\bar{\Lambda}\Lambda$ reaction are recognised: a forward rise is followed by a flat distribution.

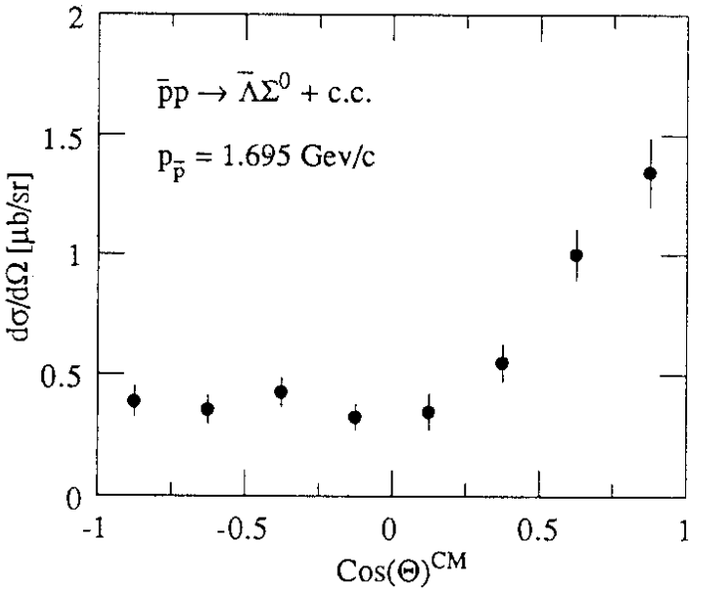

Figure 6. Differential cross section in the centre of mass for the reaction $\bar{p}p$ -> $\bar{\Lambda}\Sigma^0$+ c.c. at 1.695 GeV/c.

3.3 Polarisations and Spin Correlations

The self-analysing weak decay of the Λ-particles makes it straightforward to extract the polarisation (decay asymmetry parameter $\alpha = 0.642 \pm 0.013$). Furthermore, since the Λ and $\bar{\Lambda}$ are always detected in pairs, the spin correlations can also be obtained. The polarisation and spin correlations are analysed using the coordinate system shown in Fig. 7 via the relations

$$P_y(\Theta) = \frac{3}{\alpha_\Lambda}\frac{1}{N}\Sigma \cos(\Theta_p)$$

$$C_{ij}(\Theta) = \frac{9}{\alpha_\Lambda \alpha_{\bar{\Lambda}}}\frac{1}{N}\Sigma \cos(\Theta_p)\cos(\Theta_{\bar{p}})$$

Symmetry laws put constraints on the polarisation and spin correlation observables.

Parity conservation:
$P_x(\Theta) = P_z(\Theta) = 0$
$C_{xy} = C_{yx} = C_{yz} = C_{zy} = 0$

Charge conjugation invariance:
$P_y(\Theta) = P_{\bar{y}}(\Theta)$
$C_{ij} = C_{ji}$

CP invariance:
$\alpha_\Lambda = -\alpha_{\bar{\Lambda}}$

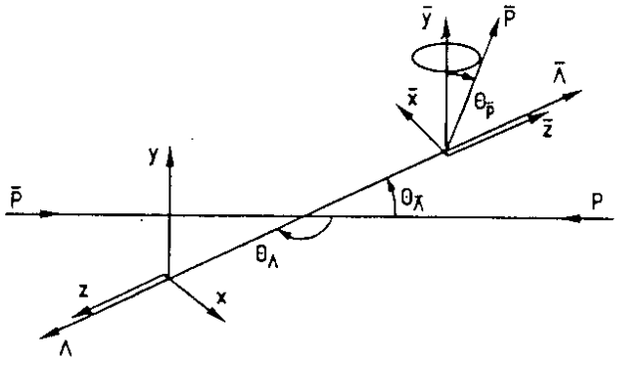

Figure 7. Coordinate system used for evaluating Λ polarisations.

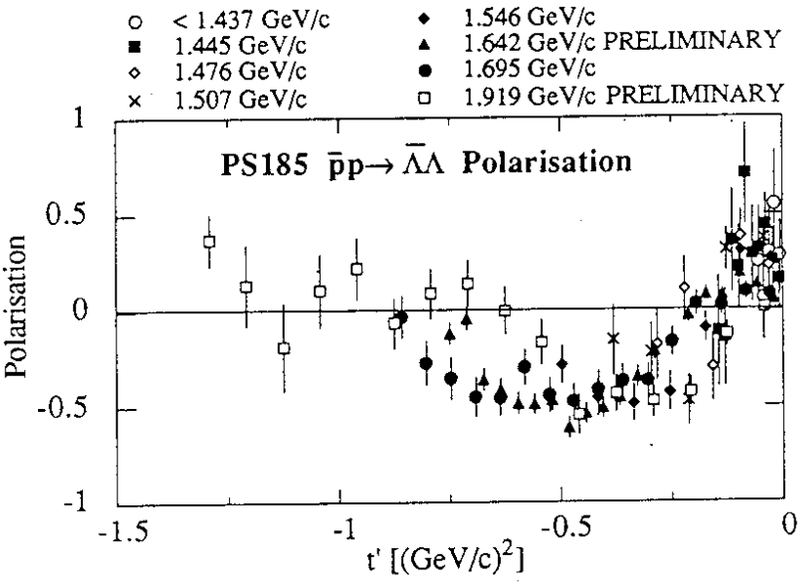

Figure 8. Polarisation as a function of t' for the reaction reaction $\bar{p}p \rightarrow \bar{\Lambda}\Lambda$ measured by PS185.

In Fig. 8 the polarisation as a function of the reduced four momentum transfer t' for the reaction $\bar{p}p \rightarrow \bar{\Lambda}\Lambda$ is shown at different momenta. Again a coherent picture emerges; the distributions become very similar. They have the common feature that the polarisation is positive at forward angles and becomes negative thereafter. In all distributions there is one zero crossing at $t' \approx -.2$ $(GeV/c)^2$, which precisely corresponds to the region of change from flat to forward rise in the differential cross section. There is probably a common source for this behaviour of the differential cross section and polarisation which, however, has yet to be understood. The only data set that differs slightly at larger t' is the one taken at $p_{\bar{p}} = 1.912$ GeV/c [8], where perhaps also a second zero crossing occurs. These data are still very preliminary and contain only 10% of the events accumulated. The polarisation of the Σ^0 in the reaction $\bar{p}p \rightarrow \bar{\Lambda}\Sigma^0$+ c.c. has been extracted at $p_{\bar{p}} = 1.695$ GeV/c [3], but it is difficult to draw conclusions from these data due to the large statistical uncertainty.

The spin correlations obtained at different momenta are shown in Fig. 9. Here again, the distributions more or less coincide on a t' scale with strong correlations in certain t' regions. Having these correlations available, the singlet fraction, S, can be calculated;

$$S = \frac{1 + C_{xx} - C_{yy} + C_{zz}}{4}$$

This quantity is a measure of the spin alignment of the produced antihyperon-hyperon system. It has the value S = 1 if the pair is produced in a relative singlet state, S = 0 if

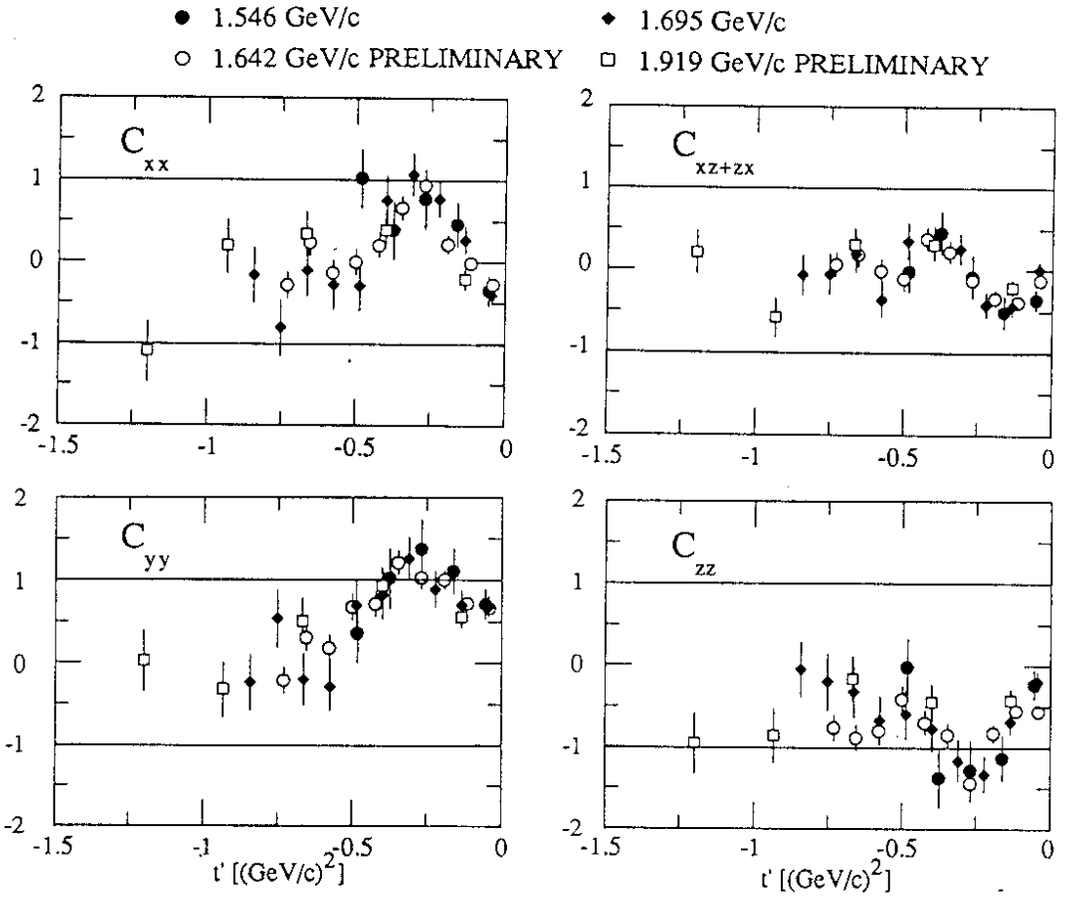

Figure 9. Spin correlations plotted as a function of t' for the reaction $\bar{p}p \rightarrow \bar{\Lambda}\Lambda$ (see text for definition).

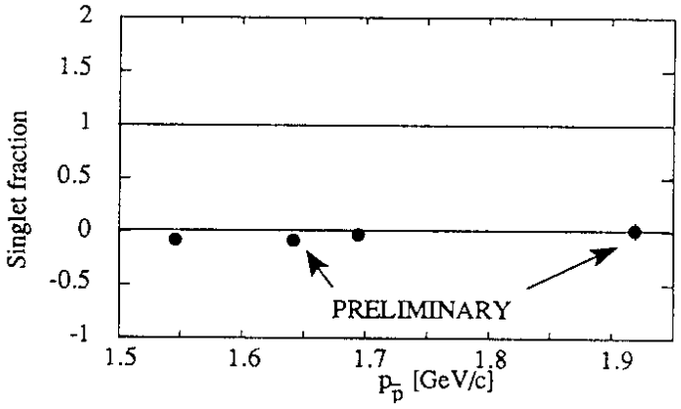

Figure 10. Avaraged value of the singlet fraction S plotted at four different momenta.

produced in a relative triplet state, and S = 0.25 for a statistical mixture of the two. In Fig. 10 the averaged singlet fraction is shown for four different momenta. It is quite clear that the $\bar{\Lambda}\Lambda$ pairs are always produced in a relative triplet state. This is in fact required from the $^3P_0$ or $^3S_1$ quark-based models. An enhanced triplet production, however, can also be understood from the relatively large importance of the tensor part of the kaon exchange potential in the boson exchange models.

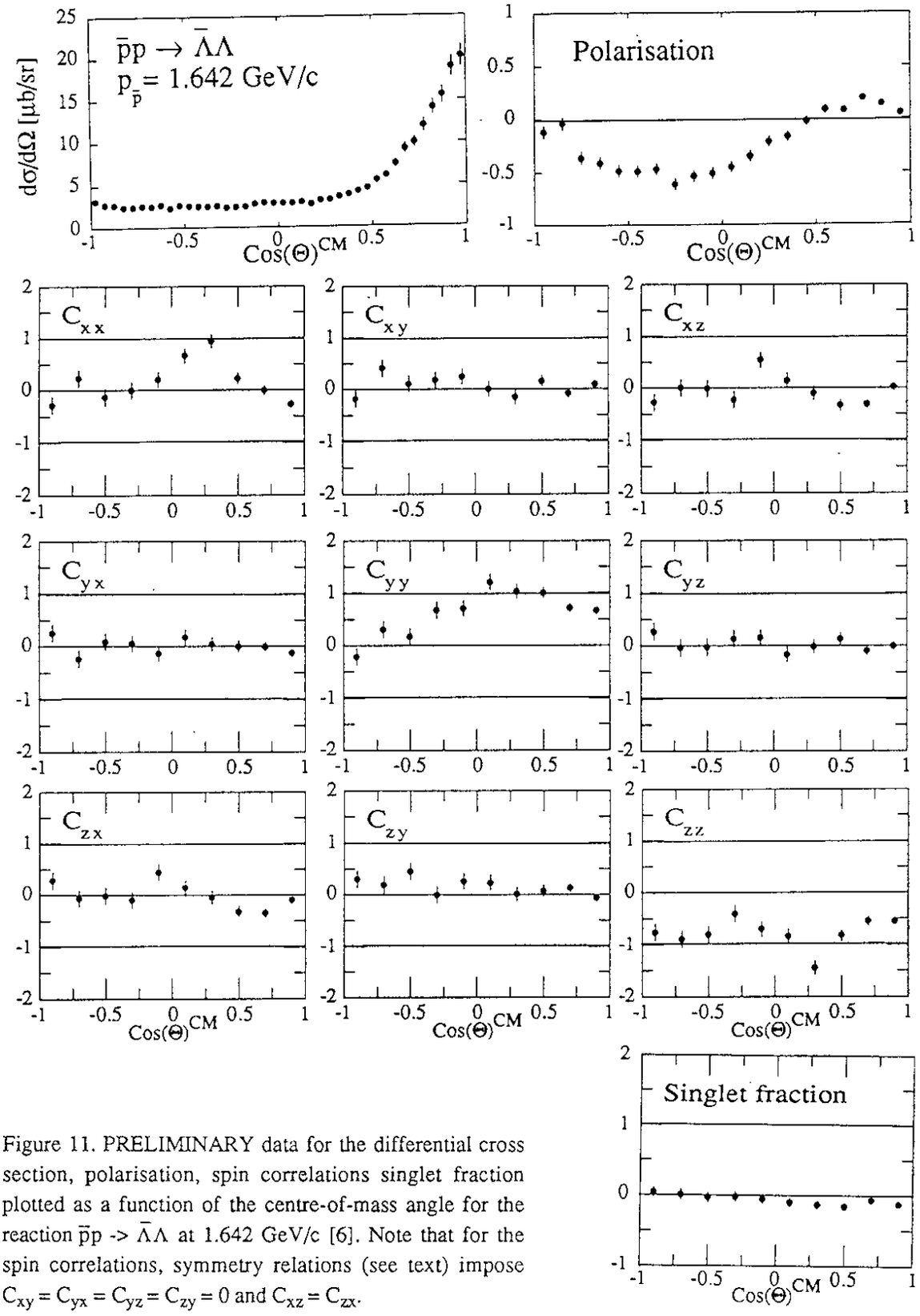

Figure 11. PRELIMINARY data for the differential cross section, polarisation, spin correlations singlet fraction plotted as a function of the centre-of-mass angle for the reaction $\bar{p}p$ -> $\bar{\Lambda}\Lambda$ at 1.642 GeV/c [6]. Note that for the spin correlations, symmetry relations (see text) impose $C_{xy} = C_{yx} = C_{yz} = C_{zy} = 0$ and $C_{xz} = C_{zx}$.

4. CONCLUSIONS

A global and coherent picture is emerging from data taken by the PS185 collaboration on the reaction $\bar{p}p \rightarrow \bar{\Lambda}\Lambda$ at momenta $p_{\bar{p}} < 2$ GeV/c.

i) Data show that $\bar{\Lambda}\Lambda$ pairs are always produced in a relative triplet state.

ii) There is a strong P-wave contribution very close to the reaction threshold.

iii) The observables $d\sigma/dt'$, P and C_{ij} are to a large extent energy independent. Plotted on a t' scale the transition from forward rise to a flat distribution in $d\sigma/dt'$ occurs at about -.2 $(GeV/c)^2$. The slope is very similar and the distributions coincide at larger t'. The polarisation is positive at small t', and turns negative for $t' > 2$ $(GeV/c)^2$. Hence, this zero crossing of the polarisations occurs at the same t' as the changeover from flat to forward rise occurs in the $d\sigma/dt'$ distributions. The polarisations taken at different $\bar{p}$ momenta look very similar, which is also true for the spin correlations.

The angular distribution obtained for the reaction $\bar{p}p \rightarrow \bar{\Lambda}\Sigma^0 +$ c.c. close to threshold looks similar to the $\bar{p}p \rightarrow \bar{\Lambda}\Lambda$ reaction.

The ratio $\sigma(\bar{\Lambda}\Sigma^0)/\sigma(\bar{\Lambda}\Lambda)$ is in fair agreement with quark model predictions, provided the comparison is made at the same excess energy.

The ensemble of data presented in this paper, in particular the new high quality data including spin correlations (see Fig. 11), should allow stringent constraints to be put on the many theoretical models, and will hopefully provide a means to distinguish between them.

ACKNOWLEDGEMENTS

These measurements reported here were only made possible by the excellent performance of the CERN antiproton complex, in particular the LEAR ring. We wish to thank the LEAR team for their enthusiasm and help.

The support from the Austrian Science Foundation, the German Federal Minister for Research and Technology, the Swedish Natural Science Research Council, the United States Department of Energy and the United States National Science Foundation is gratefully acknowledged.

REFERENCES

[1] P. D. Barnes *et al.*, Phys. Lett. **189B** (1987) 249.
[2] P. D. Barnes *et al.*, Phys. Lett. **229B** (1989) 432.
[3] P. D. Barnes *et al.*, CERN-EP/90-40, to appear in Phys. Lett. B.
[4] W. Dutty, Dissertation, Univ. of Freiburg, (1988).
[5] G. Sehl, Dissertation, Univ. of Bonn, JUEL-SPEZ-535, (1990).
[6] H. Fisher, Private communication.
[7] F. Stinzing, Private communication.
[8] M. Ziolkowski, Private communication.
[9] H. Genz and S. Tatur, Phys. Rev. **D30** (1984) 63.
[10] H. Rubinstein and H. Snellman, Phys. Lett. **165B** (1985) 187.
[11] M. Kohno and W. Weise, Preprint TPR-86-13, Contributed paper to 11th Int. Conf. on Few Body Systems in Particle and Nuclear Physics, Tokyo & Sendai, August 1986.
[12] M. Kohno and W. Weise, Phys. Lett. **176B** (1986) 15.
[13] M. Kohno and W. Weise, Nucl. Phys. **A479** (1988) 433c.
[14] S. Fururi and A. Faessler,Nucl. Phys. **A508** (1987) 669.
[15] H. Burk and M. Dillig, Phys. Rev. **C37** (1988) 1362.
[16] M. A. Alberg *et al.*, Nucl. Phys. **A508** (1990) 323c.
[17] W. Roberts,Preprint HUTP-90/A020.
[18] F. Tabakin and R.A. Eisenstein, Phys. Rev. **C31** (1985) 1857.
[19] J. A. Niskanen, Preprint Helsinki Univ HU-TFT-86-28.
[20] P. Lafrance, B. Loiseau and R. Vihn Mau, Phys. Lett. **214B** (1988) 317.
[21] P. Lafrance and B. Loiseau, Preprint CRM-1673, 1990.
[22] T. Hippchen *et al*, Proc. 4 LEAR workshop, Villars, Harwood (1988).
[23] R.G.E. Timmermans, T.A. Rijken and J.J. de Swart, Nucl. Phys. **A479** (1988) 383c.
[24] M. Kohno and W. Weise, Phys. Lett. **206B** (1988) 584.
[25] O.D. Dalkarov, K.V. Protasov and I.S. Shapiro, Preprint 37, Moscow, FIAN, 1988.
[26] A. Kudryatsev and V. Samilov, Mod. Phys. Lett. **4A** (1989) 721.
[27] W. Dutty *et al.*, Nucl. Instr. and Meth. **A253** (1986) 98.
[28] R. v. Frankenberg *et al.*, Nucl. Instr. and Meth. **A252** (1986) 570.
[29] L. Durand and J. Sandweiss, Phys. Rev. **135** (1964) B540.
[30] B. Jayet *et al.*, Il Nouvo Cimento **45A** (1978) 371.
[31] J.W. Cruz, Ph.D. thesis, Rutgers Univ., (1983).
[32] B. Y. Oh *et al.*, Nucl. Phys. **B51** (1973) 57.
[33] J. Button *et al.*, Phys. Rev. **121** (1961) 1788.
[34] P. D. Barnes *et al.*, Phys. Lett. **199B** (1987) 432.

Imprimé au CERN. Prix : 0.40 Fr.